

Strong Collective Chiroptical Response from Electric-Dipole Interactions in Atomic Systems

Marcella L. Xavier,^{1,*} Felipe A. Pinheiro,^{2,†} and Romain Bachelard^{1,‡}

¹Departamento de Física, Universidade Federal de São Carlos,

Rodovia Washington Luís, km 235 - SP-310, 13565-905 São Carlos, SP, Brazil

²Instituto de Física, Universidade Federal Rio de Janeiro, 21941-972 Rio de Janeiro, RJ, Brazil

(Dated: February 18, 2026)

Chiroptical responses in atomic systems are usually weak, as they arise from the interference between electric- and much weaker magnetic-dipole transitions. We show that atoms arranged in chiral geometries can instead exhibit a strong collective chiroptical response mediated entirely by electric-dipole interactions. Using a coupled-dipole framework, we identify a regime of pronounced chiroptical response emerging at subwavelength interatomic separations, which can be tuned by the probe frequency. This enhancement is directly linked to the formation of subradiant collective modes. Our results establish a fundamental connection between geometric chirality and collective light-matter interactions, opening new pathways for engineering and exploiting chiral optical responses in atomic systems.

Introduction. Chirality pervades nature across different length scales, from macroscopic objects to nanoscopic structures [1]. First introduced by Lord Kelvin, a chiral system is defined as one that cannot be superimposed onto its mirror image through any combination of rotations and translations [1]. Distinguishing between the two enantiomeric forms is essential in chemistry, molecular biology, and pharmaceutics, where molecular handedness critically determines the functionality of many compounds [2]. A wide range of strategies has been developed to separate and identify chiral molecules and particles, most prominently chemical methods [3]. However, these approaches are typically species-specific, often invasive, and rely on ensemble-averaged measurements. Probing chirality at the single-particle or single-molecule level remains a scientific and technological challenge due to the intrinsically weak nature of chiroptical signals [4, 5].

To address these limitations, plasmonic nanostructures have emerged as a powerful platform for enhancing chiroptical interactions by leveraging localized surface plasmon resonances [6, 7], in which intense electric multipoles can be excited [8]. Beyond plasmonics, all-dielectric, high-index nanostructures and metamaterials have attracted growing interest, as their engineered magnetic multipolar resonances enable strong interference with electric modes, providing an alternative route to enhanced chiroptical responses [8–10].

Although chiroptical enhancement in single molecules and nanoparticles is traditionally achieved through the interference of electric and magnetic multipoles, purely electric strategies are emerging as a versatile and increasingly relevant alternative in photonics [11, 12]. Beyond photonics, atomic systems are particularly well suited for realizing controlled all-electric chiral excitations owing to their resonant nature and extremely narrow linewidths, which enable precise tuning of the chiroptical response [13–16]. In addition to chiroptical enhancement, atomic chiral platforms enable nonreciprocal

directional emission [17, 18], chiral quantum optics [19], and chirality-dependent photon transport [20]. These capabilities open avenues for applications ranging from polarization control and optical logic [21] to quantum information processing [22]. Moreover, atomic systems offer direct control over collective scattering phenomena, including superradiant emission [20], further enhancing their appeal for tailoring chiral light-matter interactions.

In this work, we demonstrate that small atomic assemblies arranged in chiral geometries can exhibit pronounced chiral optical responses that are tunable over frequency variations on the order of the linewidth. Remarkably, we find that the handedness of the response can be reversed simply by adjusting the probe frequency. The resulting strong circular dichroism (CD), enabling polarization-selective transmission, originates from cooperative scattering and the associated subradiant dynamics of the system. Moreover, our analysis of the wavelength dependence shows that, for small number of atoms within the electric-dipole approximation, the contrast between right- and left-circularly polarized transmitted light is maximized in the subwavelength regime.

Chiroptical response induced by light-induced electric interactions. We consider a set of N two-level cold atoms at positions \mathbf{r}_j , driven by a weak coherent laser with Rabi frequency Ω and wavevector \mathbf{k} . Each atom is treated in the electric dipole approximation, with transition frequency ω_0 , and thus does not present chiral property itself. Under the rotating-wave and Markov approximations, the scattering dynamics is given by a set of $3N$ coupled dipole equations [23–26]:

$$\dot{\beta}_j^\zeta(t) = \left(i\Delta - \frac{\Gamma}{2} \right) \beta_j^\zeta(t) - \frac{i\Omega_\zeta}{2} e^{i\mathbf{k}\cdot\mathbf{r}_j} - \frac{\Gamma}{2} \sum_{j \neq m} \sum_{\eta} G_{\zeta,\eta}(\mathbf{r}_j - \mathbf{r}_m) \beta_m^\eta(t), \quad (1)$$

where β_j^ζ stands for the (complex) dipole components of

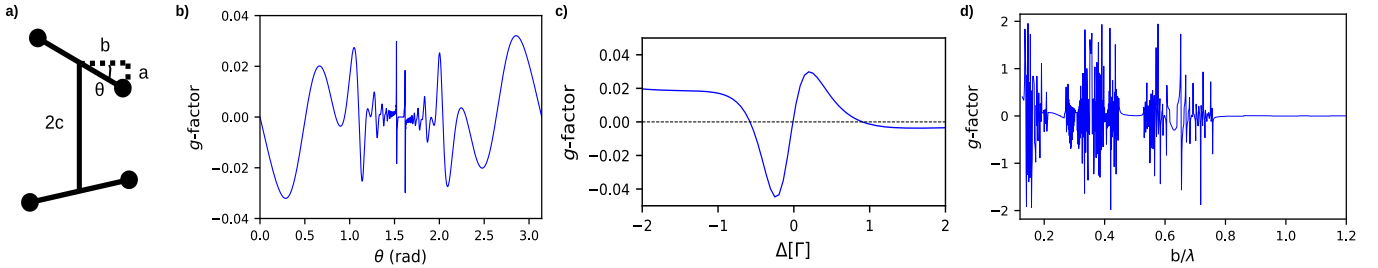


FIG. 1. a) Twisted H structure: Minimal intrinsically chiral system, with four non-coplanar atoms (electric dipoles). b) For different values of the angle one obtains distinct configurations of the structure, as evidenced by the dissymmetry factor (simulations realized for $b = 2.24/k$ and $c = 2.52/k$). c) Evolution of the CD as a function of the detuning Δ ; simulations realized for $b = 2.24/k$, $c = 2.52/k$ and $\theta = \pi/6$. d) The optical response is strongest in the subwavelengths, as shown by varying the system size. The relations between the lengths are here given by $c = 1.125b$ and $a = b \tan \theta$, with $\theta = \pi/6$.

atom j , with $\zeta \in \{-1, 0, +1\}$ referring to the polarizations $\hat{\mathbf{e}}_{\pm 1} = 1/\sqrt{2}(\mp \hat{\mathbf{x}} - i\hat{\mathbf{y}})$ and $\hat{\mathbf{e}}_0 = \hat{\mathbf{z}}$. Here, Γ is the single-atom decay rate and Δ the detuning between the laser frequency and the atomic transition.

The first right-hand term in Eq. (1) corresponds to the single-atom dynamics and the second is the driving by the external electric field, while the third one stands for the light-induced coupling between the dipoles. This set of $3N$ equations rules the evolution of the amplitudes of the induced atomic dipoles in the laser frame, and their mutual coupling is encoded in the Green's dyadic function, $G_{\zeta,\eta}(\mathbf{r})$ [27, 28]:

$$\overleftrightarrow{G}(\mathbf{r}) = \frac{3}{2} \frac{\exp(ikr)}{ikr} \left[\left(1 + \frac{i}{kr} - \frac{1}{(kr)^2} \right) \overleftrightarrow{1} + \left(-1 - \frac{3i}{kr} + \frac{3}{(kr)^2} \right) \frac{\mathbf{r} \otimes \mathbf{r}}{r^2} \right]. \quad (2)$$

In the steady state, geometrical chiral properties show up in the polarization-dependent transmission and reflection coefficients, encoded in the definition of the g -factor that characterizes CD [40, 41]:

$$g = 2 \frac{T_{\text{RCP}} - T_{\text{LCP}}}{2 - (T_{\text{RCP}} + T_{\text{LCP}})}, \quad (3)$$

where T_{RCP} and T_{LCP} are the transmission coefficients for the RCP and LCP light, respectively. The system is driven with a laser either RCP or LCP, and the corresponding transmission is computed in the forward direction as the ratio between the squared sum of the outgoing electric field (given by the sum of the incident one and that in the RCP or LCP polarization channel) and the intensity of the incident laser. The factor $g \in [-2; 2]$, with $|g| = 2$ being associated to a maximal chirality, when the system is transparent to one polarization and backscatters efficiently the opposite-handed one [42], with the sign

Note that in the single-photon (linear optics) limit considered here, the dipole dynamics (1) can be derived through a fully classical approach, treating the particles as N classical harmonic oscillators [24, 29]. Going beyond this regime to explore quantum chiral effects [22, 30–32] will require a quantum description of the atomic operators and electric field [23, 33–36]. In this work, numerical simulations were performed using the Julia package available at Ref. [37, 38].

Twisted H configuration. Let us first consider the simplest chiral system composed of $N = 4$ atoms, hereafter referred to as twisted H structure, depicted in Fig. 1(a). In order to break mirror symmetry, the parameters a , b and c must be different and non-vanishing, with dipoles arranged in the extremities of the edges [39]; the angle $\theta = \arctan(a/b)$ thus measures the deviation from the planar structure.

of the dissymmetry factor accounting for the handedness of the system.

In Fig. 1(b), we show the evolution of the g -factor with the angle θ of the twisted H structure. For $\theta = 0$ or π , the g -factor vanishes as the structure is planar, and hence achiral; otherwise it is quite sensitive to the angle. Figure 1(b) demonstrates that simple chiral systems composed of only four dipoles may already exhibit substantial dissymmetry factors. Besides, this simple chiral system illustrates how resonant scattering may be explored to control the chiroptical response. This can be appreciated in Fig. 1(c) where the sign of the g -factor changes with the detuning Δ , which can be achieved by varying the driving frequency by approximately Γ . Considering that atomic transitions can be very narrow, particularly for clock transitions, one obtains a structure in which chiroptical properties can be finely tuned, either

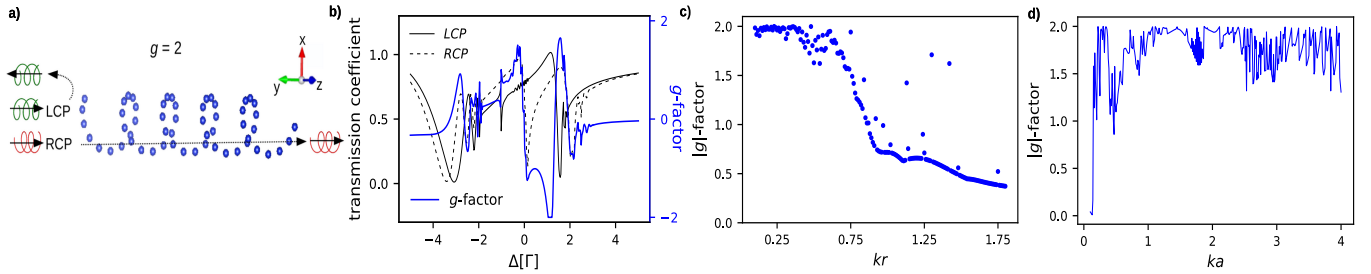


FIG. 2. (a) Representation of LCP and RCP propagating light through a helical atomic chain with right-handed helicity, all along the z -axis, for a g -factor with maximum value. (b) Transmission coefficients (black curves) for LCP (plain) and RCP (dashed) probe light, and the g -factor (blue curve), which quantifies the CD. Simulations realized for a pitch $a = 1.75/k$, radius $r = 0.5/k$, and $N = 60$ atoms, with 3 atoms per revolution. Inverted results are obtained for a left-handed helix. (c-d) g -factor as a function of the helix (c) radius and (d) pitch. While the CD is maximum for radius $r < 0.6/k$, it maintains high values for a broad range of pitches. In order to obtain these results, for each value of r and a the highest g -factor is chosen considering a broad range of Δ .

with the driving frequency or, equivalently, with shifts imposed through external fields such as the Zeeman or Stark shifts.

Finally, we notice that the chiroptical response of the twisted H is strongest when its size is smaller than the wavelength, with the g -factor going to zero when the system size is smaller than $\approx 0.8\lambda$. This can be understood as a manifestation of the $1/(kr)^2$ and $1/(kr)^3$ near-field terms in the dipole-dipole interaction (3), which couple the different polarization channels and are strongest at short scales $r < \lambda$. From a different perspective, the vanishing of the g -factor for structures larger than the wavelength corroborates the expectation that chiroptical effects in light scattering arise from multiple scattering. Specifically, a nonzero chiroptical response requires at least four scattering events, enabling the optical field to effectively probe the chirality of the system and thus ne-

cessitating a minimum of four scatterers [43].

Atomic helical structures. Motivated by the fact that the twisted H, the simplest chiral structure, already exhibits a substantial chiroptical response in light scattering from atoms, we now consider more complex configurations, such as atoms distributed along helices, the hallmark of chiral geometries. This atomic system, sketched in Fig. 2(a), is known to exhibit strong intrinsic chirality [44, 45]. Similarly to the twisted H, the transmission of RCP and LCP probe beam is very sensitive to the frequency, but also quite different for each polarization, as it can be seen Fig. 2(b). This results in a g -factor that reaches values close to ± 2 , depending on the frequency. We thus conclude that the atomic helix exhibits strong chiroptical properties, which can be tuned by varying the atomic detuning, including the sign of the g -factor.

The importance of considering subwavelengths atomic helices to enhance chiroptical effects is evidenced in Fig. 2(c), where the g -factor remains maximal for a radius $r \lesssim 0.6/k$. Large chiroptical response in the subwavelength regime is uncommon for naturally occurring small scattering systems [42], and typically require plasmonic particles arranged in typical chiral geometries such as helical assemblies of nanospheres [46], twisted nanorod dimers [47], asymmetric pyramids of chiral nanoparticles [48], or even disordered ensembles that also lack mirror symmetry [49, 50]. Here the maximum g -factor exhibits a weak dependence on the helix pitch a , with values close to 2 for a broad range of pitch values, see Fig. 2(d). In the helical case the pitch is the parameter that governs the geometrical chiral properties [39]. Note that for the smallest values of ka , the system length for the $N = 60$ dipoles becomes smaller than the wavelength, and the chiroptical response vanishes for $ka < 0.05$; in this case

the helix length becomes smaller than the wavelength.

While the above results correspond to an helix whose main axis coincides with the incident wavevector, the intrinsic chiroptical response of the structure of the structure is determined from the orientation-averaged $\langle CD \rangle_\Omega$, where $\langle \rangle_\Omega$ corresponds to an average over all possible orientations of the molecule [45]. The intrinsic chiroptical property $\langle CD \rangle_\Omega$ is of particular interest when the structures have an arbitrary orientation or no symmetry axis, such as disordered systems. Here, this average is computed by integration over 4π solid-angle, so that the system is illuminated over all possible angles. For each structure, we choose the detuning which leads to the maximum chirality. For the twisted H structure, one obtains $|\langle CD \rangle_\Omega| = 0.02$, for $\Delta = -3.60\Gamma$, which indicates a weak but nonzero intrinsic chiroptical response. For the helical structure, $|\langle CD \rangle_\Omega| = 0.12$ for $N = 60$ and $\Delta = 1.62\Gamma$, and $|\langle CD \rangle_\Omega| = 0.54$ for $N = 120$ and

$\Delta = -0.14\Gamma$, which show that a strong intrinsic chirality can be achieved for an elongated helical atomic structure.

Long-lived chiral emission. The dipole-dipole coupling leads to not only energy shifts and dispersive properties, but also a strong modification of the emission lifetime [51–61]. Aiming to study the nature of the collective modes behind the chiroptical properties, we now investigate the radiative dynamics of the system after the laser is switched off, taking as initial condition a driven steady state. As shown in Fig. 3, the forward-scattered intensity, normalized by the steady state one, first exhibits a “chiral flash” for the RCP probe, with the dynamical intensity reaching a value larger than the steady-state one. Such flash is a transient phenomenon that occurs when a close-to-resonance laser illuminating an optically thick atomic cloud, which manifests as a coherent burst of light in the forward direction [62]. Since the helical structure under consideration is right-handed by construction, with a g -factor of -0.25 , Fig. 3 shows that LCP is better transmitted than the RCP beam ($T_{LCP} > T_{RCP}$), so that the flash occurs only for the less-transmitted polarization. This shows that coherent burst of light in the forward direction is also an optical manifestation of chirality in atomic systems, henceforth dubbed chiral flash.

Furthermore, at later times the scattered intensity exhibits a much slower decay than for isolated atom, see the inset in Fig. 3. This subradiant dynamics has been reported in several platforms [63–67], with applications to storage and retrieval of light [68–71]. While it occurs both in the LCP and RCP configurations, it has a much larger amplitude in the RCP channel. This can be interpreted as the fact that the optical depth in this channel is much larger than in the LCP one [67], so the system exhibits a form of chiral subradiance. Note that subradiance is a slow radiative process distinct from multiple scattering [64, 72].

Conclusions and outlook. Detecting weak chiral signals remains a central challenge, as they often originate from the interference between electric and magnetic dipole moments, the latter typically being small. Here we show that purely electric-dipole systems can nevertheless exhibit pronounced chiroptical response, even the minimal chiral configuration composed of four atoms. Atomic assemblies of several tens of resonant emitters display strong intrinsic chirality and reach maximal g -factors. Importantly, the chiroptical response of these structures, including its sign, can be tuned either by varying the drive frequency or via externally induced level shifts. Moreover, the coexistence of superradiant and subradiant chiral modes provides a route toward controlling photon flow and storing optical information. Realizing such chiral architectures with cold atoms offers a promising pathway to combine strong chiral responses with nonlinear quantum-optical effects, for example using Rydberg-mediated interactions [73–75], enabling polarization- and photon-number-dependent scat-

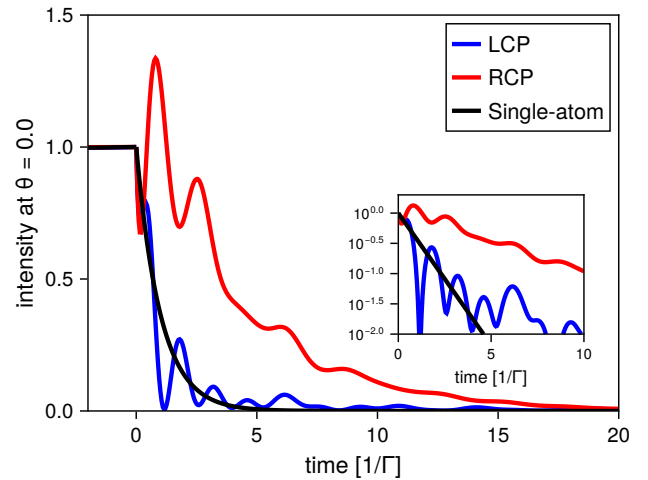


FIG. 3. Scattered intensity in a switch-off dynamics for a right-handed helix with $N = 60$, $r = 0.5/k$ and $a = 1.75/k$ at resonance, $\Delta = 0$. A “chiral flash” and a subradiant dynamics can be observed.

tering in free-space atomic arrays.

The authors acknowledge Dr. Noel A. Moreira for the fruitful discussions and support with the numerical Julia package. This study was financed, in part, by the Brazilian National Council for Scientific and Technological Development – CNPq, Grants No. 140248/2023-4 and 313632/2023-5. R. B. acknowledges the support from the São Paulo Research Foundation (FAPESP, Grants Nos. 2022/00209-6 and 2023/03300-7). F.A.P. acknowledges financial support from CAPES, CNPq, and FAPERJ.

* marcella.lx@hotmail.com

† fpinheiro@if.ufrj.br

‡ romain@ufscar.br

- [1] G. H. Wagnière, *On chirality and the universal asymmetry: reflections on image and mirror image* (John Wiley & Sons, 2007).
- [2] N. M. Maier, P. Franco, and W. Lindner, Separation of enantiomers: needs, challenges, perspectives, *Journal of Chromatography A* **906**, 3 (2001).
- [3] G. Gübitz and M. G. Schmid, Chiral separation by chromatographic and electromigration techniques. a review, *Biopharmaceutics & drug disposition* **22**, 291 (2001).
- [4] J. Kumar and L. M. Liz-Marzán, Recent advances in chiral plasmonics—towards biomedical applications, *Bulletin of the Chemical Society of Japan* **92**, 30 (2019).
- [5] M. L. Solomon, A. A. Saleh, L. V. Poulikakos, J. M. Abendroth, L. F. Tadesse, and J. A. Dionne, Nanophotonic platforms for chiral sensing and separation, *Accounts of chemical research* **53**, 588 (2020).
- [6] R. M. Kim, J.-H. Huh, S. Yoo, T. G. Kim, C. Kim, H. Kim, J. H. Han, N. H. Cho, Y.-C. Lim, S. W. Im, *et al.*, Enantioselective sensing by collective circular dichroism, *Nature* **612**, 470 (2022).

[7] Z. Liu, J. Ai, P. Kumar, E. You, X. Zhou, X. Liu, Z. Tian, P. Bouř, Y. Duan, L. Han, *et al.*, Enantiomeric discrimination by surface-enhanced raman scattering–chiral anisotropy of chiral nanostructured gold films, *Angewandte Chemie* **132**, 15338 (2020).

[8] S. Im, S. Mousavi, Y.-S. Chen, and Y. Zhao, Perspectives of chiral nanophotonics: from mechanisms to biomedical applications, *npj Nanophotonics* **1**, 46 (2024).

[9] C.-S. Ho, A. Garcia-Etxarri, Y. Zhao, and J. Dionne, Enhancing enantioselective absorption using dielectric nanospheres, *ACS Photonics* **4**, 197 (2017).

[10] J. Garcia-Guirado, M. Svedendahl, J. Puigdollers, and R. Quidant, Enhanced chiral sensing with dielectric nanoresonators, *Nano letters* **20**, 585 (2019).

[11] D. Ayuso, A. F. Ordóñez, and O. Smirnova, Ultrafast chirality: the road to efficient chiral measurements, *Phys. Chem. Chem. Phys.* **24**, 26962 (2022).

[12] D. Habibović, K. R. Hamilton, O. Neufeld, and L. Rego, Emerging tailored light sources for studying chirality and symmetry, *Nature Reviews Physics* **6**, 663–675 (2024).

[13] C. Muldoon, L. Brandt, J. Dong, D. Stuart, E. Brainis, M. Himsworth, and A. Kuhn, Control and manipulation of cold atoms in optical tweezers, *New Journal of Physics* **14**, 073051 (2012).

[14] P. Bienias, S. Subhankar, Y. Wang, T.-C. Tsui, F. Jendrzejewski, T. Tiecke, G. Juzeliūnas, L. Jiang, S. L. Rolston, J. V. Porto, and A. V. Gorshkov, Coherent optical nanotweezers for ultracold atoms, *Phys. Rev. A* **102**, 013306 (2020).

[15] H. Rivy, S. Aljunid, E. Lassalle, N. Zheludev, and D. Wilkowski, Single atom in a superoscillatory optical trap, *Communications Physics* **6** (2023).

[16] Z. Zhang, T.-W. Hsu, T. Y. Tan, D. H. Slichter, A. M. Kaufman, M. Marinelli, and C. A. Regal, High optical access cryogenic system for rydberg atom arrays with a 3000-second trap lifetime, *PRX Quantum* **6**, 020337 (2025).

[17] R. P. Cameron, A. M. Yao, and S. M. Barnett, Diffraction gratings for chiral molecules and their applications, *The Journal of Physical Chemistry A* **118**, 3472 (2014).

[18] L. Rego, O. Smirnova, and D. Ayuso, Tilting light’s polarization plane to spatially separate the ultrafast nonlinear response of chiral molecules, *Nanophotonics* **12**, 2873 (2023).

[19] D. Suárez-Forero, M. Jalali Mehrabad, C. Vega, A. González-Tudela, and M. Hafezi, Chiral quantum optics: recent developments and future directions, *Prx Quantum* **6**, 020101 (2025).

[20] J. S. Peter, S. Ostermann, and S. F. Yelin, Chirality dependent photon transport and helical superradiance, *Phys. Rev. Res.* **6**, 023200 (2024).

[21] Y. Zhang, Y. Wang, Y. Dai, X. Bai, X. Hu, L. Du, H. Hu, X. Yang, D. Li, Q. Dai, T. Hasan, and Z. Sun, Chirality logic gates, *Science Advances* **8**, 10.1126/sciadv.abq8246 (2022).

[22] P. Lodahl, S. Mahmoodian, S. Stobbe, A. Rauschenbeutel, P. Schneeweiss, J. Volz, H. Pichler, and P. Zoller, Chiral quantum optics, *Nature* **541**, 473–480 (2017).

[23] R. H. Lehmberg, Radiation from an n -atom system. i. general formalism, *Physical Review A* **2**, 883 (1970).

[24] A. A. Svidzinsky, J.-T. Chang, and M. O. Scully, Cooperative spontaneous emission of n atoms: Many-body eigenstates, the effect of virtual lamb shift processes, and analogy with radiation of n classical oscillators, *Phys. Rev. A* **81**, 053821 (2010).

[25] B. Zhu, J. Cooper, J. Ye, and A. M. Rey, Light scattering from dense cold atomic media, *Phys. Rev. A* **94**, 023612 (2016).

[26] M. O. Araújo, W. Guerin, and R. Kaiser, Decay dynamics in the coupled-dipole model, *Journal of Modern Optics* **65**, 1345 (2018).

[27] F. Pinheiro, Statistics of quality factors in three-dimensional disordered magneto-optical systems and its applications to random lasers, *Physical Review A—Atomic, Molecular, and Optical Physics* **78**, 023812 (2008).

[28] Y. A. Fofanov, A. Kuraptsev, I. Sokolov, and M. Havey, Dispersion of the dielectric permittivity of dense and cold atomic gases, *Physical Review A—Atomic, Molecular, and Optical Physics* **84**, 053811 (2011).

[29] F. Cottier, R. Kaiser, and R. Bachelard, Role of disorder in super- and subradiance of cold atomic clouds, *Physical Review A* **98**, 10.1103/physreva.98.013622 (2018).

[30] K. Ray, S. P. Ananthavel, D. H. Waldeck, and R. Naaman, Asymmetric scattering of polarized electrons by organized organic films of chiral molecules, *Science* **283**, 814 (1999).

[31] J. S. Peter, S. Ostermann, and S. F. Yelin, Chirality-induced emergent spin-orbit coupling in topological atomic lattices, *Phys. Rev. A* **109**, 043525 (2024).

[32] D. Suárez-Forero, M. Jalali Mehrabad, C. Vega, A. González-Tudela, and M. Hafezi, Chiral quantum optics: Recent developments and future directions, *PRX Quantum* **6**, 020101 (2025).

[33] N. Fayard, L. Henriet, A. Asenjo-Garcia, and D. E. Chang, Many-body localization in waveguide quantum electrodynamics, *Physical Review Research* **3**, 10.1103/physrevresearch.3.033233 (2021).

[34] S. P. Pedersen, L. Zhang, and T. Pohl, Quantum nonlinear metasurfaces from dual arrays of ultracold atoms, *Physical Review Research* **5**, 10.1103/physrevresearch.5.1012047 (2023).

[35] O. Rubies-Bigorda, S. Ostermann, and S. F. Yelin, Characterizing superradiant dynamics in atomic arrays via a cumulant expansion approach, *Physical Review Research* **5**, 10.1103/physrevresearch.5.013091 (2023).

[36] D. A. Suresh and F. Robicheaux, Emission photon statistics in collectively interacting dipole atom arrays in the low-intensity limit (2025), [arXiv:2503.16624](https://arxiv.org/abs/2503.16624).

[37] N. A. Moreira, *CoupledDipoles.jl* : a julia package for cold atoms, Instituto de Física de São Carlos, Universidade de São Paulo [doi:10.11606/T.76.2024.tde-26012024-114225](https://doi.org/10.11606/T.76.2024.tde-26012024-114225) (2024).

[38] N. A. Moreira, *CoupledDipoles.jl* (2024).

[39] A. B. Harris, R. D. Kamien, and T. C. Lubensky, Molecular chirality and chiral parameters, *Rev. Mod. Phys.* **71**, 1745 (1999).

[40] L. Cerdán, L. Zundel, and A. Manjavacas, Chiral lattice resonances in 2.5-dimensional periodic arrays with achiral unit cells, *ACS Photonics* **10** (2023).

[41] E. M. Sánchez-Carnerero, A. R. Agarrabeitia, F. Moreno, B. L. Maroto, G. Muller, M. J. Ortiz, and S. de la Moya, Circularly polarized luminescence from simple organic molecules, *Chemistry – A European Journal* **21**, 13488–13500 (2015).

[42] J. Mun, M. Kim, Y. Yang, T. Badloe, J. Ni, Y. Chen, C.-W. Qiu, and J. Rho, Electromagnetic chirality: from fundamentals to nontraditional chiroptical phenomena,

Light: Science & Applications **9**, 139 (2020).

[43] F. Pinheiro and B. A. van Tiggelen, Magnetochiral scattering of light: optical manifestation of chirality, Physical Review E **66**, 016607 (2002).

[44] L. D. Barron, True and false chirality and absolute asymmetric synthesis, *Journal of the American Chemical Society* **108**, 5539 (1986).

[45] J. Mun, M. Kim, Y. Yang, T. Badloe, J. Ni, Y. Chen, C.-W. Qiu, and J. Rho, Electromagnetic chirality: from fundamentals to nontraditional chiroptical phenomena, *Light: Science & Applications* **9**, 139 (2020).

[46] A. Kuzyk, R. Schreiber, Z. Fan, G. Pardatscher, E.-M. Roller, A. Högele, F. Simmel, A. Govorov, and T. Liedl, Dna-based self-assembly of chiral plasmonic nanostructures with tailored optical response, *Nature* **483**, 311 (2012).

[47] W. Ma, H. Kuang, L. Wang, L. Xu, W.-S. Chang, H. Zhang, M. Sun, Y. Zhu, Y. Zhao, L. Liu, C. Xu, S. Link, and N. A. Kotov, Chiral plasmonics of self-assembled nanorod dimers, *Scientific Reports* **3**, 10.1038/srep01934 (2013).

[48] W. Yan, L. Xu, C. Xu, W. Ma, H. Kuang, L. Wang, and N. A. Kotov, Self-assembly of chiral nanoparticle pyramids with strong r/s optical activity, *Journal of the American Chemical Society* **134**, 15114 (2012).

[49] V. P. Drachev, W. D. Bragg, V. A. Podolskiy, V. P. Safonov, W.-T. Kim, Z. C. Ying, R. L. Armstrong, and V. M. Shalaev, Large local optical activity in fractal aggregates of nanoparticles, *Journal of the Optical Society of America B* **18**, 1896 (2001).

[50] F. Pinheiro, V. Fedotov, N. Papasimakis, and N. I. Zhe-ludev, Spontaneous natural optical activity in disordered media, *Physical Review B* **95**, 220201 (2017).

[51] N. Skribanowitz, I. P. Herman, J. C. MacGillivray, and M. S. Feld, Observation of dicke superradiance in optically pumped hf gas, *Phys. Rev. Lett.* **30**, 309 (1973).

[52] M. Gross and S. Haroche, Superradiance: An essay on the theory of collective spontaneous emission, *Physics Reports* **93**, 301 (1982).

[53] S. Inouye, A. Chikkatur, D. Stamper-Kurn, J. Stenger, D. Pritchard, and W. Ketterle, Superradiant rayleigh scattering from a bose-einstein condensate, *Science (New York, N.Y.)* **285**, 571 (1999).

[54] M. Scheibner, T. Schmidt, L. Wörschech, A. Forchel, G. Bacher, T. Passow, and D. Hommel, Superradiance of quantum dots, *Nature Physics* **3**, 106 (2007).

[55] R. A. de Oliveira, M. S. Mendes, W. S. Martins, P. L. Saldanha, J. W. R. Tabosa, and D. Felinto, Single-photon superradiance in cold atoms, *Physical Review A* **90**, 10.1103/physreva.90.023848 (2014).

[56] M. O. Araújo, I. Krešić, R. Kaiser, and W. Guerin, Superradiance in a large and dilute cloud of cold atoms in the linear-optics regime, *Phys. Rev. Lett.* **117**, 073002 (2016).

[57] F. Jahnke, C. Gies, M. Aßmann, M. Bayer, H. Leymann, A. Foerster, J. Wiersig, C. Schneider, M. Kamp, and S. Höfling, Giant photon bunching, superradiant pulse emission and excitation trapping in quantum-dot nanolasers, *Nature Communications* **7**, 11540 (2016).

[58] D. D. Grimes, S. L. Coy, T. J. Barnum, Y. Zhou, S. F. Yelin, and R. W. Field, Direct single-shot observation of millimeter-wave superradiance in rydberg-rydberg transitions, *Phys. Rev. A* **95**, 043818 (2017).

[59] A. Kuraptsev, I. Sokolov, and M. Havey, Angular distribution of single photon superradiance in a dilute and cold atomic ensemble, *Physical Review A* **96** (2017).

[60] Z. Wang, H. Li, W. Feng, X.-H. Song, C. Song, W. Liu, Q. Guo, X. Zhang, H. Dong, D. Zheng, H. Wang, and D. Wang, Controllable switching between superradiant and subradiant states in a 10-qubit superconducting circuit, *Physical Review Letters* **124** (2020).

[61] W. Guerin, Super- and subradiance in dilute disordered cold atomic samples: observations and interpretations, in *Advances in Atomic, Molecular, and Optical Physics* (Elsevier, 2023) p. 253–296.

[62] M. Chalony, R. Pierrat, D. Delande, and D. Wilkowski, Coherent flash of light emitted by a cold atomic cloud, *Phys. Rev. A* **84**, 011401 (2011).

[63] A. S. Kuraptsev and I. M. Sokolov, Spontaneous decay of an atom excited in a dense and disordered atomic ensemble: Quantum microscopic approach, *Phys. Rev. A* **90**, 012511 (2014).

[64] P. Weiss, M. O. Araújo, R. Kaiser, and W. Guerin, Subradiance and radiation trapping in cold atoms, *New Journal of Physics* **20**, 063024 (2018).

[65] R. Pennetta, D. Lechner, M. Blaha, A. Rauschenbeutel, P. Schneeweiss, and J. Volz, Observation of coherent coupling between super- and subradiant states of an ensemble of cold atoms collectively coupled to a single propagating optical mode, *Phys. Rev. Lett.* **128**, 203601 (2022).

[66] X.-L. Chu, V. Angelopoulou, P. Lodahl, and N. Rotenberg, Subradiant states for two imperfect quantum emitters coupled by a nanophotonic waveguide, *Phys. Rev. A* **106**, 053702 (2022).

[67] W. Guerin, A. Michelle, and R. Kaiser, Subradiance in a large cloud of cold atoms, *Physical Review Letters* **116** (2015).

[68] G. Facchinetto, S. D. Jenkins, and J. Ruostekoski, Storing light with subradiant correlations in arrays of atoms, *Phys. Rev. Lett.* **117**, 243601 (2016).

[69] R. Holzinger, D. Plankensteiner, L. Ostermann, and H. Ritsch, Nanoscale coherent light source, *Phys. Rev. Lett.* **124**, 253603 (2020).

[70] J. Rui, D. Wei, A. Rubio-Abadal, S. Hollerith, J. Zeiher, D. M. Stamper-Kurn, C. Gross, and I. Bloch, A subradiant optical mirror formed by a single structured atomic layer, *Nature* **583**, 369–374 (2020).

[71] G. Ferioli, A. Glicenstein, L. Henriet, I. Ferrier-Barbut, and A. Browaeys, Storage and release of subradiant excitations in a dense atomic cloud, *Phys. Rev. X* **11**, 021031 (2021).

[72] Y. A. Fofanov, I. M. Sokolov, R. Kaiser, and W. Guerin, Subradiance in dilute atomic ensembles: Role of pairs and multiple scattering, *Phys. Rev. A* **104**, 023705 (2021).

[73] M. Moreno-Cardoner, D. Goncalves, and D. E. Chang, Quantum nonlinear optics based on two-dimensional rydberg atom arrays, *Phys. Rev. Lett.* **127**, 263602 (2021).

[74] L. Zhang, V. Walther, K. Mølmer, and T. Pohl, Photon-photon interactions in Rydberg-atom arrays, *Quantum* **6**, 674 (2022).

[75] L. Zhang, F. Yang, K. Mølmer, and T. Pohl, Unidirectional quantum-optical elements for waveguide-qed with subwavelength rydberg-atom arrays in free space, *Optica Quantum* **3**, 256 (2025).